RESEARCH ARTICLE

In-situ formation of nitrogen doped microporous carbon nanospheres derived from polystyrene as lubricant additives for anti-wear and friction reduction

Yixin WANG[1], **Qi LU**[1], **Huijie XIE**[1], **Shujuan LIU**[1], **Qian YE**[1,*], **Feng ZHOU**[1,2,*], **Weimin LIU**[1,2]

[1] *State Key Laboratory of Solidification Processing, Center of Advanced Lubrication and Seal Materials, School of Materials Science and Engineering, Northwestern Polytechnical University, Xi'an 710072, China*

[2] *State Key Laboratory of Solid Lubrication, Lanzhou Institute of Chemical Physics, Chinese Academy of Sciences, Lanzhou 730000, China*

Abstract: This study presents a nitrogen-doped microporous carbon nanospheres (N@MCNs) prepared by a facile polymerization–carbonization process using low-cost styrene. The N element *in situ* introduces polystyrene (PS) nanospheres via emulsion polymerization of styrene with cyanuric chloride as crosslinking agent, and then carbonization obtains N@MCNs. The as-prepared carbon nanospheres possess the complete spherical structure and adjustable nitrogen amount by controlling the relative proportion of tetrachloromethane and cyanuric chloride. The friction performance of N@MCNs as lubricating oil additives was surveyed utilizing the friction experiment of ball-disc structure. The results showed that N@MCNs exhibit superb reduction performance of friction and wear. When the addition of N@MCNs was 0.06 wt%, the friction coefficient of PAO-10 decreased from 0.188 to 0.105, and the wear volume reduced by 94.4%. The width and depth of wear marks of N@MCNs decreased by 49.2% and 94.5%, respectively. The carrying capacity of load was rocketed from 100 to 400 N concurrently. Through the analysis of the lubrication mechanism, the result manifested that the prepared N@MCNs enter clearance of the friction pair, transform the sliding friction into the mixed friction of sliding and rolling, and repair the contact surface through the repair effect. Furthermore, the tribochemical reaction between nanoparticles and friction pairs forms a protective film containing nitride and metal oxides, which can avert direct contact with the matrix and improve the tribological properties. This experiment showed that nitrogen-doped polystyrene-based carbon nanospheres prepared by *in-situ* doping are the promising materials for wear resistance and reducing friction. This preparing method can be ulteriorly expanded to multi-element co-permeable materials. Nitrogen and boron co-doped carbon nanospheres (B,N@MCNs) were prepared by mixed carbonization of N-enriched PS and boric acid, and exhibited high load carrying capacity and good tribological properties.

Keywords: lubricant additives; hypercrosslinked polystyrene; carbon nanospheres; friction reduction; anti-wear

1 Introduction

In industrial production, friction and wear can lead to mechanical wear and energy consumption. Hence, lubricant is necessary to protect machinery from wear and maintain surface quality [1]. It is well recognized that the base oil used alone is not able to meet the promoted requirements under extreme conditions. In this regard, adding functional additives is deemed as one of the most universal and facile means to enhance the comprehensive properties of base oil [2, 3]. Nanoparticles, such as metal [4, 5], metal oxide [6, 7], sulfide [8], carbon [9–11] and so on, can effectively improve properties of friction and enhance the

load-carrying capacity of base oil due to size effect, colloidal effect, protective film, and third body effects [1, 3]. In previous studies, TiO_2 nanoparticles as lubricating oil additives can reduce the friction coefficient of base oil by 85% through bearing effect and repair effect [7]. Cu as nano-additives greatly improved the friction properties of lubricating oil through the protective film effect, and the friction coefficient was reduced by 17.3%–23.6% [4].

Carbon ball has received much more attention in the field of lubrication. Due to the unique physical and chemical properties, carbon ball can significantly improve the friction properties of base oil [12]. Panickar et al. have synthesized carbon spheres using noncatalytic CVD method, the as-prepared carbon spheres displayed good tribological properties due to rolling friction, and the friction coefficient of the neat oil reduced by 11% with addition of 0.3 wt% of carbon spheres [13]. The carbon spheres with abundant functional groups were prepared by hydrothermal carbonization method, which as additives reduced the friction coefficient and wear rate by 33.2% and 24.2% respectively [14].

Carbon nanomaterials have gathered great interests in the past several decades as nano-lubricant additives, however, carbon nanomaterials always accumulate spontaneously in lubricating oil owing to their high surface energy, resulting in poor dispersion stability, which is fatal for lubrication effect and long-term usability of hybrid lubricants. According to the research, the lubrication performance of carbon spheres could be boosted by doping a variety of elements including sulfur, phosphorus, nitrogen, and boron [15–17] due to the high reactivity brought by heteroatom. Xiong et al. have prepared SiO_2-reinforced B–N-co-doped reduced graphene oxide via microwave-synthesis method, which displayed eminent load-carrying, anti-wear, and anti-friction performance as additives [18]. The S, N co-doped carbon nanoparticle (S,N-CN) were prepared via hydrothermal reaction, the as-obtained S,N-CN exhibited good lubricating performance compared to base oil PEG200 when playing the role as lubricating additives [17].

Polystyrene (PS) is one of the best known synthetic polymers, which is easily manufactured by the free radical polymerization of styrene. PS has been of great practical value in many diversified fields attributable to its enduring stability, low cost, and convenience of fabrication. Carbon nanomaterials prepared via carbonization of PS have been explored thoroughly to serve various application scenarios. Nie et al. synthesized carbon material by carbonizing waste polystyrene and CCl_4 as raw materials [19]. Whereas, the common pyrolysis of polystyrene can only obtain undoped carbon nanomaterials, which limits extended properties and further functionalization. Consequently, doping active heteroatom by introducing foreign source during preparation, such as S, P, N, B, is usually used as an effective mean to alter the intrinsic properties of carbon materials. Chen et al. have prepared sulfur-doped hard carbon by carbonizing mixture of PS spheres and sulfur powders under nitrogen atmosphere [20]. At present, tramp element doping of carbon materials can be well realized via various methods such as hydrothermal method, activation method, post-processing method, chemical vapor deposition, etc. [21]. Herein, we have successfully prepared N@MCNs via a facile polymerization–carbonization process using low-cost styrene. Abundant N atoms were *in situ* introduced into polystyrene (PS) nanospheres via emulsion polymerization of styrene with cyanuric chloride as crosslinking agent, and then the crosslinking PS nanospheres could be further carbonized to obtain N@MCNs. The as-prepared N@MCNs gained more regular spherical structure and adjustable nitrogen amount by controlling the relative proportion of tetrachloromethane and cyanuric chloride. The tribological performances of base oil PAO-10 abound with all kinds of N@MCNs, were assessed remarkably under extreme test conditions. As oil-based lubricating additives, the as-prepared N@MCNs displayed outstanding friction reduction and anti-wear abilities with a trace amount addition in PAO-10 through rolling effect, polishing effect, repairing effect, and protective film effect. The mean COF of PAO-10 containing 0.06 wt% N@MCNs decreased to 0.105 and the wear volume reduced by 94.4%. The load-carrying ability increased from 100 to 400 N. The preparation method provided can be further expanded to obtain multi-element co-permeable materials, the N and B co-doped carbon nanospheres were prepared triumphantly by mixed carbonization

of N-enriched PS and boric acid, the tribological performance of which were studied in detailed.

2 Experimental

2.1 Preparation of hypercrosslinked polystyrene nanospheres (HPSs)

Polystyrene nanospheres were prepared by homopolymerization of styrene. Specific production process referred to the previous literature [22]. For synthesis of HPSs, 0.5g PS and 0.37g cyanuric chloride was dispersed in 30 mL tetrachloromethane and 25 mlmethylene chloride, respectively, and the two solutions were mixed well together. 1.4 g anhydrous aluminium chloride was added to initiate polymerization. The reaction was carried out at 75 °C for 24 h under 300 rpm. The relative content of tetrachloromethane and cyanuric chloride was changed for the preparation of CHPSs, HPSs-1, HPSs-2, HPSs-3, and THPSs. The specific content is shown in Table S1 in the Electronic Supplementary Material (ESM).

2.2 Preparation of nitrogen doped microporous carbon nanospheres (N@MCNs)

In the first place, 0.2 g CHPSs was added into 60 mL deionized water, which was heated to 185 °C in 100 mL Teflon valve sealing cartridge for 6 h in order to avoid serious agglomeration of particles during carbonization. CMCNs was synthesized by carbonizing the samples after hydrothermal pretreatment at 500 °C for 5 h under nitrogen atmosphere. The production process of N@MCNs-1, N@MCNs-2, N@MCNs-3, and TMCNs was the same as that of CMCNs, where HPSs-1,

HPSs-2, HPSs-3, and THPSs were used as raw materials, respectively.

2.3 Preparation of boron, nitrogen co-doped microporous carbon nanospheres (B,N@MCNs)

100 mg hydrothermal-pretreated samples were mixed with 200 mg boric acid under uniform stirring for one hour. Above mixture were placed in the tubular furnace at 550 °C for 5 h at nitrogen atmosphere. B,N@MCNs were obtained by washing the carbonized samples with pure water at 70 °C and then drying under vacuum at 45 °C, in order to remove residual boron oxide.

The materials and characterization methods used in the experiment are provided in the ESM.

3 Results and discussions

Scheme 1 shows the production process of microporous carbon nanospheres. Carbon-crosslinked bridges and triazine-crosslinked bridges are formed between benzene rings by using tetrachloromethane and cyanuric chloride as crosslinking agents, respectively. The morphology characteristics of microporous carbon nanospheres were shown in Fig. 1. CMCNs, N@MCNs-1, N@MCNs-2, and N@MCNs-3 all showed perfect spherical structure, while the spherical structure of TMCNs collapsed obviously, indicating that carbon tetrachloride, as a crosslinking agent, can improve the structural stability of carbon nanospheres and inherit nanostructure during carbonization. EDS mappings of N@MCNs-2 (Figs. 1(f)–1(h)) exhibited a well-proportioned distribution of N elements, which is signifying that nitrogen was successfully doping
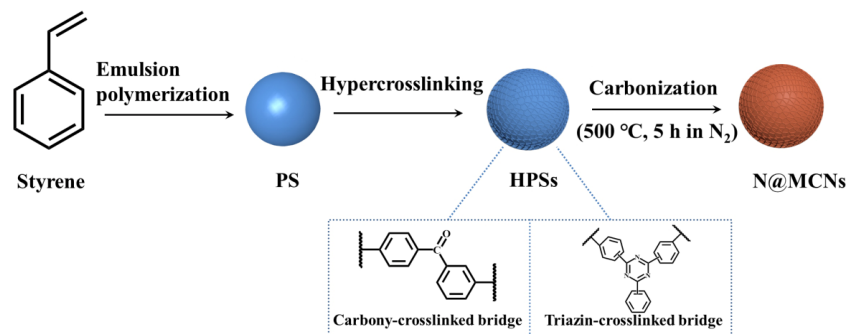
Scheme 1 Schematic diagram of preparation nitrogen doped microporous carbon nanomaterials as nanoadditives for PAO-10 lubricants.
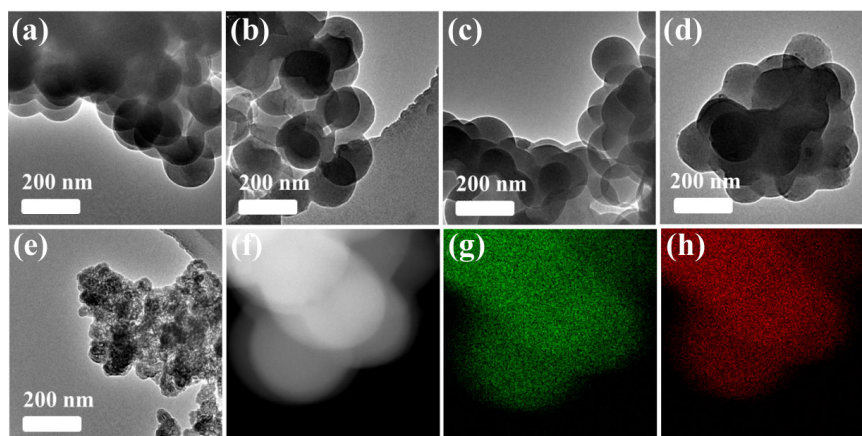
Fig. 1 TEM images of (a) CMCNs, (b) N@MCNs-1, (c) N@MCNs-2, (d) N@MCNs-3, and (e) TMCNs. (f) HAADF image of N@MCNs-2, (g) N elemental mapping, and (h) C elemental mapping of N@MCNs-2.

into the carbon nanospheres with a homogeneous distribution.

The FT-IR spectrum was used for ulteriorly certifying the formation of carbon-crosslinked bridge and triazine-crosslinked bridges (Fig. S1 in the ESM). The peaks can be observed at 1,666 cm^{-1} in CMCNs, N@MCNs-1, N@MCNs-2, and N@MCNs-3 in comparison with the spectrum of TMCNs, which fully proved the triumphant formation of crosslinking C=O bridges [23]. The characteristic peaks of 1,510 and 1,387 cm^{-1} appeared at N@MCNs-1, N@MCNs-2, N@MCNs-3, and TMCNs, corresponding to the stretching vibration peak of triazinyl, which are not detected in the CMCNs [24]. The alteration of pore structure caused by crosslinking agent was assessed by N_2 adsorption–desorption isotherms. Nitrogen absorption of CMCNs, N@MCNs-1, N@MCNs-2 and N@MCNs-3 sharply increased at P/P_0 <0.1, indicating that abundant micropores existed in samples, which was not observed in TMCNs (Fig. S2 in the ESM). The Brunauer–Emmett–Teller surface area (S_{BET}) of CMCNs, N@MCNs-1, N@MCNs-2, and N@MCNs-3 were 374.5, 323.8, 416.4, and 389.5 $m^2 \cdot g^{-1}$ respectively, while the value of TMCNs decreased to 16.3 $m^2 \cdot g^{-1}$, which is due to the collapse of TMCNs structure during carbonization (Table S2 in the ESM). The results further prove that carbon nanospheres possess the structural stability and inherit nanostructure due to formation of carbon-crosslinked bridges. For purpose of analyzing the surface chemical composition of the prepared samples, the XPS of the samples was carried out. Figure S3 in the ESM shows the full XPS

survey spectra of CMCNs, N@MCNs-1, N@MCNs-2, N@MCNs-3, and TMCNs. Obvious nitrogen signal was observed in N@MCNs-1, N@MCNs-2, N@MCNs-3, and TMCNs, which is not detected in CMCNs. It can be concluded from XPS analysis that nitrogen was introduced *in situ* into carbon nanospheres by forming the triazine-crosslinked bridge with cyanuric chloride as a crosslinking agent. Table S3 in the ESM summarizes the surface chemical composition data of carbon nanospheres prepared with different adding amounts of tetrachloromethane and cyanuric chloride. The nitrogen content of carbon nanospheres increased with the augment of the addition of cyanuric chloride, which is due to the increasement of triazine-crosslinked bridges between benzene rings. As shown in Fig. 2(a), the binding energy of the C 1s of N@MCNs-2 at 284.7, 286.1, and 288.8 eV was attributed to the C–C/C=C, C–O/C–N, and C=O, which coincided with the O 1s peaks (Fig. 2(c)) of 533.5 eV (C–O) and 532.1 eV (C=O), respectively [25]. The signal at 288.8 eV indicated the C=O crosslinking bridge between benzene rings, which is ascribed to CCl_4 acting as the crosslinking agent. The peaks at 400.4 eV (pyridinic N) and 399.2 eV (pyrrolic N) are deemed to deconvoluted N 1s peak (Fig. 2(b)) [22, 26].

Graphitization and structural defects of the N@MCNs were analyzed by the Raman spectra. As shown in Fig. 2(d), the intensity of D (1,346 cm^{-1}) and G (1,595 cm^{-1}) peaks of N@MCNs decreased with the augment of nitrogen doping amount. The D band manifests the existence of amorphous carbon and surface defects of N@MCNs, and the G band
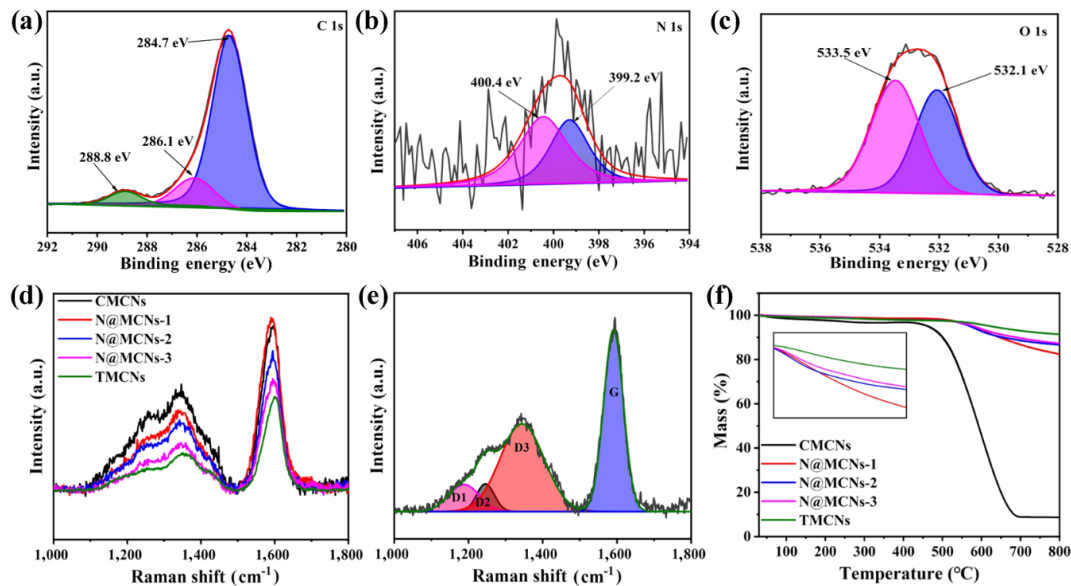
Fig. 2 (a) C 1s, (b) N 1s, and (c) O 1s XPS spectra of N@MCNs-2. (d) Raman spectra of sample, (e) Raman analysis of N@MCNs-2. (f) TG curves of sample.

represents characteristic crystalline graphite which is corresponding to highly graphitized carbon with the high intension of the G band [27]. In order to further research defect density of N@MCNs, the intensity ratio of D/G band was surveyed (Table S4 in the ESM), which implies the density of defects and the disorder extent in the structure [28]. With the increase of nitrogen content, the I_D/I_G ratio decreased, indicating that the void defects of carbon nanospheres decreased and the graphitization degree increased, which may be attributed to the structural instability of the triazine-crosslinked bridge during the carbonization process. The peaks (Fig. 2(e)) could be fit into four peaks (D1, D2, D3, and G in the vicinity of 1,188, 1,246, 1,345, and 1,595 cm^{-1}, respectively). The D1 and D3 peaks originate from sp^3-rich phase of disordered amorphous carbon and the A$_{1g}$ symmetry mode of disordered graphitic lattice located at the edges of the graphene layer, respectively. Whereas the D2 band is related to the C–C and C=C stretching vibrations or the A$_{1g}$ symmetry mode of the disordered graphitic lattice [27, 29]. The G band is attributed to sp^2 carbon atoms in a hexagonal lattice with E$_{2g}$ symmetry [17]. As shown in Fig. 2(f) and Table S5 in the ESM, thermogravimetric (TG) analysis showed that the weight loss rates of N@MCNs-1, N@MCNs-2, N@MCNs-3, and TMCNs were 17.6, 13.3, 12.7, and 8.6 wt%, respectively, whereas CMCNs established a 91.3 wt%

weight loss within the limits of 30–800 °C. The result suggested that the thermal stability of carbon nanospheres was improved, which may be attributed to the formation of triazine-crosslinking bridges between benzene rings. Dispersive stability (Fig. S4 in the ESM) of nanoparticles in base oil is the critical factor impacting properties of tribology. With the increase of nitrogen content, the suspension of carbon nanomaterials seemed more stable gradually. The carbon nanomaterials (N@MCNs-2 and N@MCNs-3) remained stable in suspension for five days because the lipophilic functional groups in nitrogen-doped carbon nanospheres improved the dispersion stability. On the contrary, obvious reunion particles of TMCNs could be viewed flowing and precipitating in the bottom of bottle only after 1 days under the same ultrasonic time, which was caused by the collapse of TMCNs carbonization structure, thus resulting in serious particle aggregation.

The tribological properties of N@MCNs as oil-based lubricant additives were evaluated firstly under constant conditions. As shown in Fig. S5 in the ESM, sharp increase in the coefficient of friction took place under circumstance of lubricating by PAO-10 at about 50 s, causing violent seizure between two tribopairs. This phenomenon occurred because the volume of the friction pair is much larger than the contact peak point, the temperature of peak point will drop rapidly when

separated from the contact point, as a consequence, the protective film like the lubricating oil film and adsorption film covering the worn surface will break instantly in this state, making the contacting peak point stick, and then the adhesion node will be destroyed in the sliding process, resulting in serious wear. Expectedly, the COF of lubricants containing N@MCNs decreased significantly compared with base oil, N@MCNs-2 and N@MCNs-3 (Figs. S5(a) and S5(b) in the ESM) showed eminent performance of reducing friction and anti-wear because of forming the protective film. However, the COF of TMCNs seemed to be unstable from the beginning of test, which may be caused by the poor dispersion induced stacking of nanospheres. It is well known that whether superfluous or inadequate nano-additives in PAO-10 will lead to worsen performance of lubrication. In order to improve its commercial value, N@MCNs-2 was selected as lubricating oil additive for further analysis and research. Therefore, the concentration effect of N@MCNs-2 (Fig. 3) was examined via tracing the COF versus time at different addition (0.1 to 0.02 wt%). The lubricating oil of 0.06 wt% N@MCNs-2 performed optimum. Comparing to base oil, the mean COF of PAO-10 containing 0.06 wt% N@MCNs-2 decreased from 0.188 to 0.105 (Fig. 3(a)), and the wear

volume reduced from 9.12×10^5 to 0.51×10^5 μm^3 (Fig. 3(d)). The additive is insufficient to cover the contact surface when the additive amount was under 0.06 wt%, resulting in direct collisions of friction pairs. However, when the addition amount is greater than 1.0 wt%, nanoparticles were prone to aggregate and deposit in the base oil, which could lead to inferior friction performance. In order to further explore the performance improvement brought by carbon nanomaterials as additives, the tribological tests of HPSs-2 and N@MCNs-2 were conducted. In comparison with HPSs-2, the mean COF of PAO-10 containing 0.06 wt% N@MCNs-2 decreased from 0.15 to 0.11 (Fig. 3(b)), and the wear volume reduced from 3.34×10^5 to 0.51×10^5 μm^3 (Fig. 3(e)). The sectional profiles show the width and depth of the wear scars depicted in Fig. 3(c) and Fig. S(6) in the ESM. Compared with the base oil, the width and depth of wear scar decreased by 49.2% and 94.5 %, respectively, after adding 0.06 wt% of the N@MCNs-2 and decreased by 22.0% and 91.0%, respectively, compared with HPSs. Similar results were obtained from the 3D contour morphology results of worn surfaces (Fig. 3(f)). The lower disk lubricated by PAO-10 showed apparent scratches and grooves, mainly due to adhesive wear. The exterior morphology of wear scar was not obviously modified,
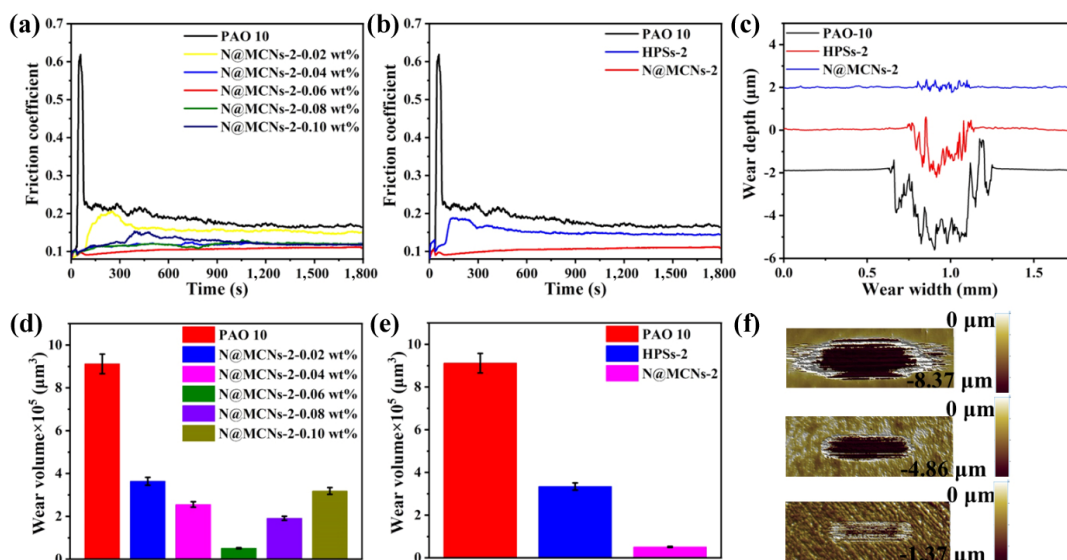

Fig. 3 (a) COF curve of N@MCNs-2 with different concentration. (b) COF curve of different lubricants with concentrations of 0.06 wt% sample. (c) Wear scar section profile of lower disks under different lubricants. (d) Wear of footwall under different lubricating oil. (e) Wear of footwall under different lubricants with concentrations of 0.06 wt% sample. (f) 3D contour morphology results of worn surfaces lubricated by PAO-10 (top), PAO-10 + 0.06 wt% HPSs-2 (middle), and PAO-10 + 0.06 wt% N@MCNs-2 (bottom). The experiments of friction were evaluated under constant conditions (50 °C, 150 N, 25 Hz, 1 mm).

but the depth of the furrows could be mildly shallower after adding of HPSs. Scratches and furrows were dramatically lessened with the addition of N@MCNs-2 thanks to the forming of protective film, proving that the effects of N@MCNs as lubricant additives on reducing friction and wear resistance occured simultaneously. That also may be attributed to the additives of carbon nanomaterials bringing more solid compounds forming on the surface [3].

Figure 4 displays the lubrication properties of nano-additives under different conditions (under variational loads and frequencies). Under the frequency gradient from 5 to 40 Hz, PAO-10 and PAO-10 containing 0.06 wt% HPSs (Fig. 4(a)) showed early lubrication failure, while the utilizing N@MCNs-2 as additives can maintain the correspondingly lower COF in the vicinity of 0.097. Figure 4(b) depicts that PAO-10 containing 0.06 wt% HPSs showed the load carrying capacity of 150 N, while that with N@MCNs-2 possessed the higher load capacity from 100 to 400 N compared to pure base oil. COF of base oil increases markedly along with the increase of load, when the load is lower than 400 N, the lubricant with nano-additives always maintains a low friction coefficient. When greater than 400 N, the friction coefficient increases sharply. This is because COF of the base oil is related to the normal load. When the nanoparticles are added, COF of the lubricant becomes less dependent on the normal load [30]. When the load is higher than 400 N, the friction coefficient increases sharply because the rolling friction of nanoparticles is limited [31]. Under the synergism of ball bearing effect and protective film effect, the load resistance of N@MCNs-2 is obviously improved.

The formation mechanism of friction film on worn surface was discussed. Raman spectra of three points on the scar surface were taken for analysis to detect the chemical binding of the worn surface lubricated by PAO-10 with 0.06 wt% N@MCNs-2 as shown in Fig. S7 in the ESM. The characteristic D and G bands (1,346 and 1,595 cm^{-1}) of the carbon material were required on the surface of the wear scar as similar with the as-prepared carbon nanospheres, indicating the formation of carbon film [32]. As shown in Fig. S8 in the ESM, the uniform protective film took shape on the surface of the abrasion mark, and the element types and classification of the friction film are further observed by EDS (Fig. S8(c) in the ESM). The friction film mainly composed of metal oxides and carbon-nitrogen compounds was formed on the surface of the steel matrix. At the same time, carbon signal is clearly observed in the friction film region, indicating the formation of carbon film during the friction process [32, 33]. The detailed composition of carbon film on wear surface was further evaluated by XPS spectrum in Fig. 5. The C 1s spectrum peaks at 284.8 and 288.1 eV put down to C−C/C=C and C=O, which rooted from the organic section in N@MCNs-2 adsorbed on the surface of wear scar. The peaks of N 1s at 400.1 eV and the peak of C 1s at 286.0 eV suggested the formation of carbonitride in the tribo-chemical reaction [34], which is consistent with the results of Raman and FIB-TEM. The peaks of Fe 2p at 712.6 and 710.3 eV can be identified as Fe 2p3/2 for Fe_2O_3, Fe 2p3/2 for Fe_3O_4 respectively, which coincided with the O 1s peaks of 531.8 and 530.0 eV [17, 35, 36]. Ultimately, the results show that under the effects of physical adsorption and tribo-chemical reaction, the composite
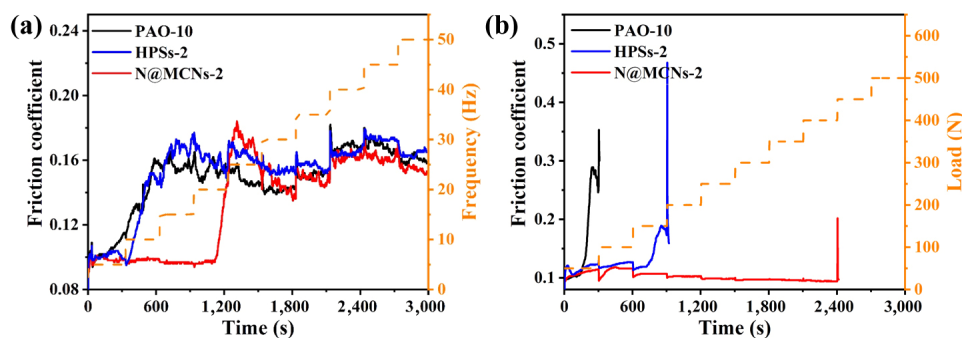

Fig. 4 (a) COF of different lubricating oil under variable frequency conditions (150 N, 50 °C, and the frequency ramp test from 5 to 50 Hz at 5 Hz/5 min). (b) COF under extreme pressure (50 °C, 25 Hz, and the load ramp test from 50 to 500 N at 50 N/5 min). Concentrations of nano-additives were 0.06 wt%.
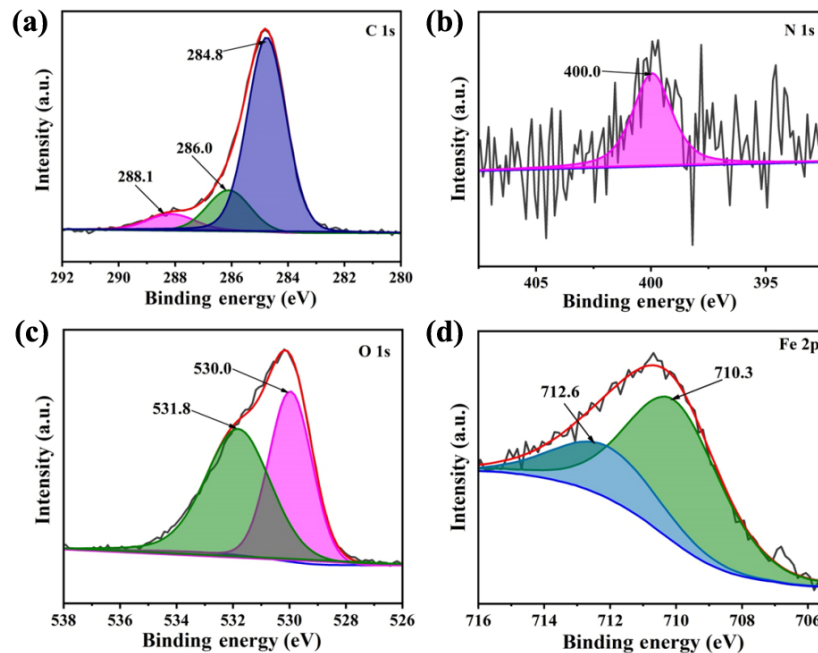
Fig. 5 XPS spectra of wear scar based PAO-10 + 0.06 wt% N@MCNs-2 under constant conditions: (a) C 1s, (b) N 1s, (c) O 1s, (d) Fe 2p.

protective film with iron oxide and carbon and nitrogen compounds was formed on the wear surface.

The experimental method can prepare multi-element co-doped carbon materials by mixed carbonization. B,N@MCNs were successfully prepared via mixed carbonization of HPSs-2 and boric acid. Faultless sphericity was exposed in SEM (Fig. S9(a) in the ESM) and TEM (Fig. S9(b) in the ESM) images of B,N@MCNs-2, indicating that the spherical structures of carbon nanospheres have been barely affected by mixing boric acid into carbonization. High-resolution XPS spectra of B,N@MCNs-2 (Fig. S10 in the ESM) emerged the undetected boron signal in N@MCNs-2, verifying that boron is doped into carbon nanospheres successfully (doping boron content is 0.83 at%) (Table S6 in the ESM). As shown in Fig. S11 and Table S7 in the ESM, the graphitization degree and structural defects of B,N@MCNs-2 are sightly changed comparing with N@MCNs-2. In order to further explore the tribological properties of B,N@MCNs-2, the COF curves of B,N@MCNs-2 at different concentrations of 0.1–0.02 wt% were showed in Fig. 6. The result showed that PAO-10 with 0.04 wt% B,N@MCNs-2 possessed the best lubricating performance. The mean COF of PAO-10 containing 0.04 wt% B,N@MCNs-2 decreased from 0.188 to 0.100 (Fig. 6(a)) and wear volume reduced from 9.12×10^5 to 0.60×10^5 μm^3

(Fig. 6(d)) comparing with the base oil. To distinguish the improvement effect between B,N@MCNs-2 and N@MCNs-2, contrast tribological tests were carried out. Compared with PAO-10 containing 0.04 wt% N@MCNs-2, the COF of PAO-10 containing 0.04 wt% B,N@MCNs-2 decreased from 0.117 to 0.100 (Fig. 6(b)), and the wear volume reduced from 2.56×10^5 to 0.60×10^5 μm^3 (Fig. 6(e)). Similar results were shown in 3D contour morphology results of worn surfaces in Fig. 6(c) that there were fewer scratches and furrows with 0.04 wt% B,N@MCNs-2. Compared with the base oil, the width and depth of wear scar of B,N@MCNs-2 decreased by 44.4% and 91.9% respectively, while compared with N@MCNs-2, decreased by 6.0% and 85.1% respectively, which can be ascribed to the involvement of boron in forming the more effective protective film (Fig. S12 in the ESM). To extend its application, the tribological properties of B,N@MCNs-2 under varying loads are analyzed in detail. Figure 6(e) depicted that the B,N@MCNs-2 extends the load resistance from 100 to 600 N compared with PAO-10.

The chemical bonding of carbon film on B,N@MCNs-2-based wear surface was further evaluated by XPS spectrum. Figure 7(a) depicted that the peaks of the deconvolution C 1s spectrum at 288.5, 286.6, 285.3, and 284.6 eV are attributed to C=O, C=N, C–O/C–N/C–B and C=C, respectively, coinciding
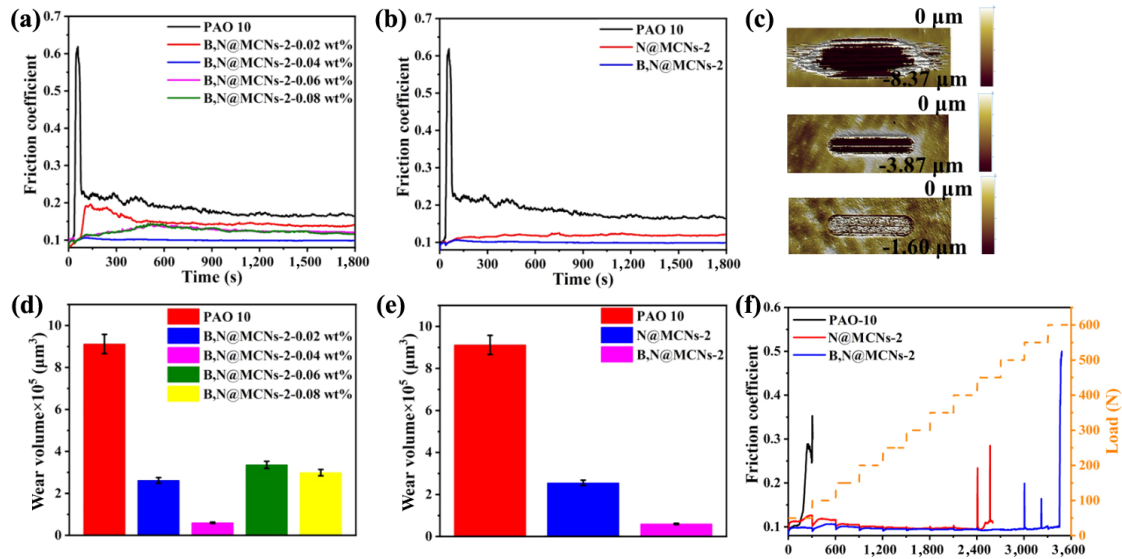
Fig. 6 (a) COF curve of B,N@MCNs-2 with different concentration under constant conditions. (b) COF curve of different lubricants with 0.04 wt% sample under constant conditions. (c) 3D contour morphology results of worn surfaces lubricated by PAO-10 (top), PAO-10 + 0.04 wt% N@MCNs-2 (middle) and PAO-10 + 0.04 wt% B,N@MCNs-2 (bottom). (d) Wear volume of lower disks based B,N@MCNs-2 under different concentrations. (e) Wear volumes of lower disks based different sample with concentrations of 0.04 wt% sample. (f) Curve of COF under extreme pressure (50 °C, 25 Hz, and the load carrying test from 50 to 600 N at 50 N/5 min).
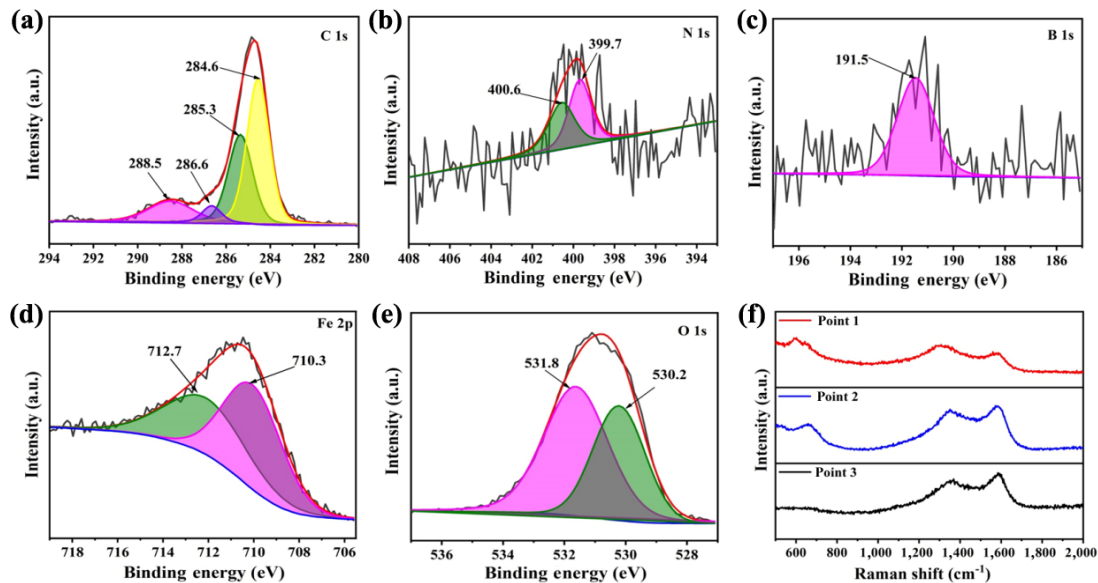

Fig. 7 XPS spectra of wear scar based PAO-10 + 0.04 wt% B,N@MCNs-2 under constant conditions: (a) C 1s, (b) N 1s, (c) B 1s, (d) Fe 2p, (e) O 1s. (f) Raman spectra of wear surface.

with the N 1s peaks of 399.7 and 400.6 eV as well as the B 1s peak of 191.5 eV, which were derived from the organic section in B,N@MCNs-2 adsorbed on the wear scar and the formation of carbonic nitride compound and carbonic boron compound in the tribo-chemical reaction [16, 25]. The peaks of Fe 2p at 712.7 and 710.3 eV can be identified as Fe 2p3/2 for Fe_2O_3, Fe 2p3/2 for Fe_3O_4 respectively, which coincided

with the O 1s peaks of 531.8 and 530.2 eV [35, 36]. Finally, the results manifested that the complex protective film took shape with the synergetic effects of physical adsorption and tribo-chemical reaction on the worn surface, primarily composing of iron oxide, carbonic nitride compound, and carbonic boron compound [37, 38].

To sum up, the lubrication mechanism of N@MCNs
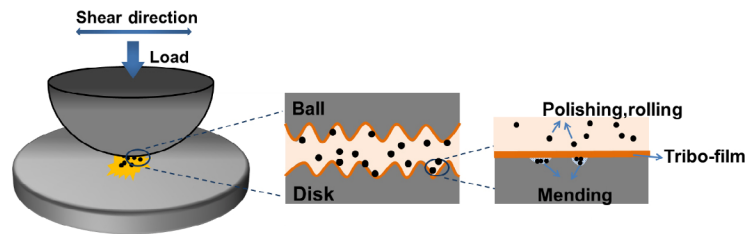
Scheme 2 Anti-wear and anti-friction mechanism of N@MCNs as nano-additives in base oil.

as lubricant additives are provide by Scheme 2 in-depth analysis. Nano-additives possess suitable size to enter contact asperities, excellent thermal stability, variety of particle chemistries, and active reaction ability with the surface without an induction period. The prepared N@MCNs can enter the clearance of the friction pair, transform the sliding friction into the mixed friction of sliding and rolling, and polish the surface of the friction pair, which are called rolling effect and polishing effect, respectively. Carbon nanospheres also deposit the uneven surface grooves and surface of the friction pair was repaired by repairing effect under the action of radial force. Furthermore, the as-obtained N@MCNs are able to form an effective protective film through tribo-chemical reactions between N@MCNs and the iron substrate. The protective films composed of nitrides and metal oxides can prevent the tribo-pairs from direct crash and endow remarkable lubricating performance. Based on the above analysis, N@MCNs as lubricant additive can create miraculous promotion on the anti-wear and anti-friction of the PAO-10.

4   Conclusions and outlook

We have provided a simple method for the *in-situ* preparation of N-doped carbon nanospheres via emulsion polymerization and subsequent carbonization using low-cost styrene. The as-prepared carbon nanospheres possessing superior spherical structure and more suitable nitrogen content were obtained by controlling the relative proportion of tetrachloromethane and cyanuric chloride. As oil-based lubricating additive, the as-prepared N@MCNs displayed excellent friction reduction and wear resistance abilities with a trace amount addition in the PAO-10 base oil through rolling effect, polishing effect, repair effect, and protective film effect. The COF of PAO-10 containing 0.06 wt%

N@MCNs decreased from 0.188 to 0.105 and the wear volume reduced by 94.4%, while the width and depth of wear scars were diminished by 49.2% and 94.5% respectively. Moreover, the load carrying ability of PAO-10 increased from 100 to 400 N. This preparation method can be further developed into multi-element co-permeable materials. Nitrogen and boron co-doped carbon nanospheres were prepared by mixed carbonization of N-enriched PS and boric acid. The load-carrying ability of hybrid oil ulteriorly increased to 600 N and the COF decreased to 0.100 when 0.04 wt% of the B,N@MCNs was added. What we have done in this work not only puts forward a kind of novel oil-based lubricating additives, but also broadens the horizons of the fabrication of co-doped carbon nanomaterials to supply other applications.

Acknowledgements

Declaration of competing interest

The authors have no competing interests to declare that are relevant to the content of this article. The authors Feng ZHOU and Weimin LIU are the Editorial Board Members of this journal.

Electronic Supplementary Material

Supplementary material is available in the online version of this article at https://doi.org/10.1007/s40544-023-0766-2.

Commons Attribution 4.0 International License, which permits use, sharing, adaptation, distribution and reproduction in any medium or format, as long as you give appropriate credit to the original author(s) and the source, provide a link to the Creative Commons licence, and indicate if changes were made.

The images or other third party material in this article are included in the article's Creative Commons licence, unless indicated otherwise in a credit line to the material. If material is not included in the article's Creative Commons licence and your intended use is not permitted by statutory regulation or exceeds the permitted use, you will need to obtain permission directly from the copyright holder.

To view a copy of this licence, visit http://creativecommons.org/licenses/by/4.0/.

References

[1] Shahnazar S, Bagheri S, Abd Hamid S B. Enhancing lubricant properties by nanoparticle additives. *Int J Hydrog Energy* **41**(4): 3153–3170 (2016)

[2] Dai W, Kheireddin B, Gao H, Liang H. Roles of nanoparticles in oil lubrication. *Tribol Int* **102**: 88–98 (2016)

[3] Ali I, Basheer A, Kucherova A, Memetov N, Pasko T, Ovchinnikov K, Pershin V, Kuznetsov D, Galunin E, Grachev V, et al. Advances in carbon nanomaterials as lubricants modifiers. *J Mol Liq* **279**: 251–266 (2019)

[4] Ali M K A, Hou X J, Abdelkareem M A A. Anti-wear properties evaluation of frictional sliding interfaces in automobile engines lubricated by copper/graphene nanolubricants. *Friction* **8**(5): 905–916 (2020)

[5] Cui Y H, Xue S H, Chen X, Bai W, Liu S J, Ye Q, Zhou F. Fabrication of two-dimensional MXene nanosheets loading Cu nanoparticles as lubricant additives for friction and wear reduction. *Tribol Int* **176**: 107934 (2022)

[6] Zhao J H, Yang G B, Zhang Y J, Zhang S M, Zhang C L, Gao C P, Zhang P Y. Controllable synthesis of different morphologies of CuO nanostructures for tribological evaluation as water-based lubricant additives. *Friction* **9**(5): 963–977 (2021)

[7] Patil H H, Pawar G B, Mali P V, Ballal Y P, Gondkar V S. Enhancement of tribological properties by adding titanium dioxide (TiO$_2$) nanoparticles in mineral based SN-500 oil. *Mater Today Proc* **59**: 128–133 (2022)

[8] Xu Y, Hu E Z, Hu K H, Xu Y F, Hu X G. Formation of an adsorption film of MoS$_2$ nanoparticles and dioctyl sebacate on a steel surface for alleviating friction and wear. *Tribol Int* **92**: 172–183 (2015)

[9] Cui Y H, Xue S H, Wang S Y, Chen X, Liu S J, Ye Q, Zhou F, Liu W M. Fabrication of carbon dots intercalated MXene hybrids via laser treatment as oil-based additives for synergistic lubrication. *Carbon* **205**: 373–382 (2023)

[10] Yang H M, Li J S, Zeng X Q. Tribological behavior of nanocarbon materials with different dimensions in aqueous systems. *Friction* **8**(1): 29–46 (2020)

[11] Wu P, Chen X C, Zhang C H, Zhang J P, Luo J B, Zhang J Y. Modified graphene as novel lubricating additive with high dispersion stability in oil. *Friction* **9**(1): 143–154 (2021)

[12] He T X, Chen N C, Fang J H, Cai G X, Wang J, Chen B S, Liang Q L. Micro/nano carbon spheres as liquid lubricant additive: Achievements and prospects. *J Mol Liq* **357**: 119090 (2022)

[13] Panickar R, Sobhan C B, Chakravorti S. Investigations on tribological properties of non-catalytic CVD synthesized carbon spheres in lubricant. *Diam Relat Mater* **106**: 107834 (2020)

[14] Wu C W, Wei C X, Jin X, Akhtar R, Zhang W. Carbon spheres as lubricant additives for improving tribological performance of polyetheretherketone. *J Mater Sci* **54**(6): 5127–5135 (2019)

[15] Ye Q A, Liu S, Xu F, Zhang J, Liu S J, Liu W M. Nitrogen-phosphorus codoped carbon nanospheres as lubricant additives for antiwear and friction reduction. *ACS Appl Nano Mater* **3**(6): 5362–5371 (2020)

[16] Jaiswal V, Kalyani, Umrao S, Rastogi R B, Kumar R, Srivastava A. Synthesis, characterization, and tribological evaluation of TiO$_2$-reinforced boron and nitrogen co-doped reduced graphene oxide based hybrid nanomaterials as efficient antiwear lubricant additives. *ACS Appl Mater Interfaces* **8**(18): 11698–11710 (2016)

[17] Wang B B, Hu E Z, Tu Z Q, David K D, Hu K H, Hu X G, Yang W, Guo J H, Cai W M, Qian W L, *et al.* Characterization and tribological properties of rice husk carbon nanoparticles Co-doped with sulfur and nitrogen. *Appl Surf Sci* **462**: 944–954 (2018)

[18] Xiong S, Zhang B S, Luo S, Wu H, Zhang Z. Preparation, characterization, and tribological properties of silica-nanoparticle-reinforced B-N-co-doped reduced graphene oxide as a multifunctional additive for enhanced lubrication. *Friction* **9**(2): 239–249 (2021)

[19] Nie T M, Yuan Z Y, Yin S, Tu W R, Yan W L, Gao J J, Jiang X M. Thermal behavior of crosslinking polystyrene resin to carbon material by one-step carbonization. *J Porous Mater* **27**(1): 249–261 (2020)

[20] Chen X Y, Cheng X B, Liu Z G. High sulfur-doped hard carbon anode from polystyrene with enhanced capacity and

stability for potassium-ion storage. *J Energy Chem* **68**: 688–698 (2022)

[21] Ke P, Zeng D, Xing H, Cui J, Li X, Qin R. Research progress of nitrogen-doped modified carbon materials. *Appl Chem Ind* **49**: 1818−1822 (2020)

[22] Wang Y X, Zhang T T, Qiu Y Q, Guo R S, Xu F, Liu S J, Ye Q, Zhou F. Nitrogen-doped porous carbon nanospheres derived from hyper-crosslinked polystyrene as lubricant additives for friction and wear reduction. *Tribol Int* **169**: 107458 (2022)

[23] Ouyang Y, Shi H M, Fu R W, Wu D C. Highly monodisperse microporous polymeric and carbonaceous nanospheres with multifunctional properties. *Sci Rep* **3**: 1430 (2013)

[24] Qiu Y, Liu Q, Han H, Yu T, Wang H, Xu F. Design and preparation of polystyrene-based porous polymers with triazine crosslinker. *J Funct Polym* **33**: 554−562 (2020)

[25] Liu B, Chen H B, Yang M, Liu Y J, Li H M. Flexible solid-state supercapacitors with outstanding capacitive performance enabled by N/B-codoped porous carbon nanosheets. *ACS Appl Energy Mater* **4**(8): 7552–7561 (2021)

[26] Oyama K, Seike M, Mitamura K, Watase S, Suzuki T, Omura T, Minami H, Hirai T, Nakamura Y, Fujii S. Monodispersed nitrogen-containing carbon capsules fabricated from conjugated polymer-coated particles via light irradiation. *Langmuir* **37**(15): 4599–4610 (2021)

[27] Sahoo B N, Kandasubramanian B. Photoluminescent carbon soot particles derived from controlled combustion of camphor for superhydrophobic applications. *RSC Adv* **4**(22): 11331–11342 (2014)

[28] Poh H L, Šimek P, Sofer Z, Pumera M. Sulfur-doped graphene *via* thermal exfoliation of graphite oxide in H_2S, SO_2, or CS_2 gas. *ACS Nano* **7**(6): 5262–5272 (2013)

[29] Xue S H, Cui Y H, Chen X, Shi J Q, Liu S J, Ye Q, Zhou F. Zwitterionic dopamine sulfonate functionalized carbon quantum dots as water-based lubricant additive for friction and wear reduction. *Appl Surf Sci* **615**: 156411 (2023)

[30] Lee K, Hwang Y, Cheong S, Choi Y, Kwon L, Lee J, Kim S H. Understanding the role of nanoparticles in nano-oil lubrication. *Tribol Lett* **35**(2): 127–131 (2009)

[31] Rudge R E D, Theunissen K, Stokes J R, Scholten E, Dijksman J A. Tribology of hard particles lubricating soft surfaces. *Phys Rev Materials* **5**(5): 055604 (2021)

[32] Lu Q, Zhang T T, He B L, Xu F, Liu S J, Ye Q, Zhou F. Enhanced lubricity and anti-wear performance of zwitterionic polymer-modified N-enriched porous carbon nanosheets as water-based lubricant additive. *Tribol Int* **167**: 107421 (2022)

[33] Wen P, Lei Y Z, Yan Q Q, Han Y Y, Fan M J. Multilayer tribofilm: An unique structure to strengthen interface tribological behaviors. *ACS Appl Mater Interfaces* **13**(9): 11524–11534 (2021)

[34] Shang W J, Ye M T, Cai T, Zhao L N, Zhang Y X, Liu D, Liu S G. Tuning of the hydrophilicity and hydrophobicity of nitrogen doped carbon dots: A facile approach towards high efficient lubricant nanoadditives. *J Mol Liq* **266**: 65–74 (2018)

[35] Gao J D, Du C F, Zhang T T, Zhang X Z, Ye Q A, Liu S J, Liu W M. Dialkyl dithiophosphate-functionalized $Ti_3C_2T_x$ MXene nanosheets as effective lubricant additives for antiwear and friction reduction. *ACS Appl Nano Mater* **4**(10): 11080–11087 (2021)

[36] He B L, Liu S, Zhao X Y, Liu J X, Ye Q A, Liu S J, Liu W M. Dialkyl dithiophosphate-functionalized gallium-based liquid-metal nanodroplets as lubricant additives for antiwear and friction reduction. *ACS Appl Nano Mater* **3**(10): 10115–10122 (2020)

[37] Zhang T T, Liu S, Zhang X Z, Gao J D, Yu H, Ye Q A, Liu S J, Liu W M. Fabrication of two-dimensional functional covalent organic frameworks *via* the thiol-ene "click" reaction as lubricant additives for antiwear and friction reduction. *ACS Appl Mater Interfaces* **13**(30): 36213–36220 (2021)

[38] Ye Q, Liu S, Zhang J, Xu F, Zhou F, Liu W M. Superior lubricity and antiwear performances enabled by porous carbon nanospheres with different shell microstructures. *ACS Sustainable Chem Eng* **7**(14): 12527–12535 (2019)
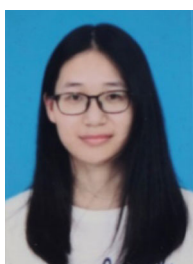
Yixin WANG. She received her B.E. degree in Huaqiao University, China (2020). She is currently a master student in School of Materials Science and Engineering at Northwestern Polytechnical University (NWPU). Her research interest is porous carbon nanospheres as lubricant additives.

Qian YE. He is an associate professor at Northwestern Polytechnical University. He got his Ph.D. degree in organic chemistry at Lanzhou University (2010). He spent one year (2013–2014) at Université catholique de Louvain as a research associate. His research interests focus on functional nanomaterials, anti-fouling materials, and lubricant coating. He has published more than 80 papers with a current h-index of 32.

Feng ZHOU. He is a full professor in Lanzhou Institute of Chemical Physics, Chinese Academy of Sciences, China, and the director of State Key Laboratory of Solid Lubrication. He got his Ph.D. degree in 2004 and spent three years (2005–2008) in University of Cambridge as a research associate. He has been published more than 300 peer-reviewed papers with h-index of 88. His research interests include the bioinspired tribology, drag-reduction and antibiofouling, and functional coatings. He has gained one National Award for Natural Sciences (the second class), and serves as an editorial board member of *Tribology International*, *Journal of Fiber Bioengineering and Informatics*, etc.